

Birefringence compensated AWG demultiplexer with angled star couplers

Tingting Lang, Jian-Jun He, Jing-Guo Kuang, and Sailing He

State Key Laboratory of Modern Optical Instrumentation, Centre for Optical and Electromagnetic Research, Zhejiang University, Hangzhou, PR China 310058

jjhe@zju.edu.cn

Abstract: A new approach to birefringence compensation in arrayed waveguide gratings (AWG) is proposed. The star couplers are designed according to Rowland circle construction with an oblique incident/diffraction angle, similar to the case of an echelle grating. Such an AWG design is more general and flexible, and the conventional AWG becomes its special case when the grating angle is zero. By appropriately designing the star coupler shape, the birefringence of the arrayed waveguides can be compensated by that of the slab waveguides. The details of the design method and simulation results are presented.

©2007 Optical Society of America

OCIS codes: (130.3120) Integrated optics devices; (230.7390) Waveguides, planar.

References and links

1. H. Takahashi, Y. Hibino, and I. Nishi, "Polarization-insensitive arrayed waveguide grating wavelength multiplexer on silicon," *Opt. Lett.* **17**, 499-501 (1992).
2. J. B. D. Soole, M. R. Amersfoort, H. P. Leblanc, N. C. Andreadakis, A. Rajhel, C. Caneau, M. A. Koza, R. Bhat, C. Youtsey, and I. Adesida, "Polarization-independent InP arrayed waveguide filter using square cross-section waveguides," *Electron. Lett.* **32**, 323-324 (1996).
3. J. H. den Besten, M. P. Dessens, C. G. P. Herben, X. J. M. Leijtens, F. H. Groen, M. R. Leys and M. K. Smit, "Low-Loss, compact, and polarization independent PHASAR demultiplexer fabricated by using a double-etch process," *IEEE Photon. Technol. Lett.* **14**, 62-64 (2002).
4. N. Yurt, K. Rausch, A. Kost and N. Peyghambarian, "Design and fabrication of a broadband polarization and temperature insensitive arrayed waveguide grating on InP," *Opt. Express* **13**, 5535-5541 (2005).
5. Y. Yoshikuni, "Semiconductor arrayed waveguide gratings for photonic integrated devices," *IEEE J. Sel. Top. Quantum Electron.* **8**, 1102-1114 (2002).
6. H. Takahashi, Y. Hibino, Y. Ohmori, and M. Kawachi, "Polarization-insensitive arrayed-waveguide wavelength multiplexer with birefringence compensating film," *IEEE Photon. Technol. Lett.* **5**, 707-709 (1993).
7. M. Zirngibl, C. H. Joyner and P. C. Chou, "Polarisation compensated waveguide grating router on InP," *Electron. Lett.* **31**, 1662-1664 (1995).
8. J.-J. He, B. Lamontagne and E. S. Koteles, "Polarisation dispersion compensated AWG demultiplexer fabricated in a single shallow etching step," *Electron. Lett.* **35**, 737-738 (1999).
9. S. M. Ojha, *et al.*, "Simple method of fabricating polarization insensitive and very low crosstalk AWG grating devices," *Electron. Lett.* **34**, 78-79 (1998).
10. Y. Inoue, M. Itoh, Y. Hashizume, Y. Hibino, A. Sugita, and A. Himeno, "A novel birefringence compensating AWG design," *OFC 2001*, WB4-1 (2001).
11. W. N. Ye, D.-X. Xu, S. Janz, P. Cheben, M.-J. Picard, B. Lamontagne, N. G. Tarr, "Birefringence control using stress engineering in silicon-on-insulator (SOI) waveguides," *J. Lightwave Technol.* **23**, 1308-1318 (2005).
12. J.-J. He, E. S. Koteles, B. Lamontagne, L. Erickson, A. Delage, and M. Davies, "Integrated polarization compensator for WDM waveguide demultiplexers," *IEEE Photon. Technol. Lett.* **11**, 224-226 (1999).
13. M. K. Smit and C. Van Dam, "PHASAR-based WDM-devices: principles, design and applications," *IEEE J. Sel. Top. Quantum Electron.* **2**, 236-250 (1996).
14. K. Okamoto, *Fundamentals of Optical Waveguides* (New York: Academic Press), 30-38.

1. Introduction

Polarization dependence is an important issue in planar waveguide based wavelength (de)multiplexers for DWDM applications. For a conventional arrayed waveguide grating (AWG) based device, owing to the difference in the propagation constants of the TE (transverse electric) and TM (transverse magnetic) modes in planar waveguides, a polarization dependent wavelength shift ($PD\lambda$) occurs in the spectral responses. Several approaches have been developed to compensate the $PD\lambda$, including the insertion of a half wave plate in the middle of the arrayed waveguides [1], non-birefringence waveguide design [2-5], different waveguides in a triangular shaped patch area of the AWG [6, 7], and the integration of a polarization compensator in the slab region [8]. All those techniques suffer from problems ranging from fabrication complexities to poor performance, or they are limited to specific structures and material systems. For silica based AWGs, a common method is to use doped silica in the upper cladding [9]. However, this would degrade the long term stability and reliability of the device, and requires accurate control of the doping levels.

Another approach is to utilize birefringence dependence on the core width and introduce two different core widths in the arrayed waveguides [10]. The drawback of this approach is that it introduces coupling loss between different waveguides and the core width difference is limited due to multimode concern. In this paper, we present a new design method for eliminating the birefringence of AWGs. By utilizing the birefringence difference between the slab waveguides and the arrayed waveguides, a polarization insensitive AWG can be realized without requiring any additional fabrication step or two different channel waveguides.

2. Principle of the birefringence compensation in AWGs

In silica-on-silicon based material system, it has been observed experimentally and verified theoretically that the stress-induced birefringence is dependent on waveguide width [10] and is significantly higher in slab waveguides than in channel waveguides when the same layer structure and doping are used. Figure 1 shows the calculated birefringence $\Delta n = n_{TE} - n_{TM}$ as a function of the thermal expansion coefficient of the upper cladding, which is related to the doping levels in commonly used boron phosphorus silicate glass (BPSG) [9]. A buried channel waveguide with a core size of $6\mu\text{m} \times 6\mu\text{m}$ and a slab waveguide of the same core height are used as an example. The theoretical model of Ref. [11] is used and the thermal expansion coefficient of the silicon substrate is assumed to be $3.60 \times 10^{-6}/\text{K}$ [11]. One can see that there is a considerable difference between the birefringence of the channel waveguide and the slab waveguide. This difference is the basis of the birefringence compensation method presented in this paper.

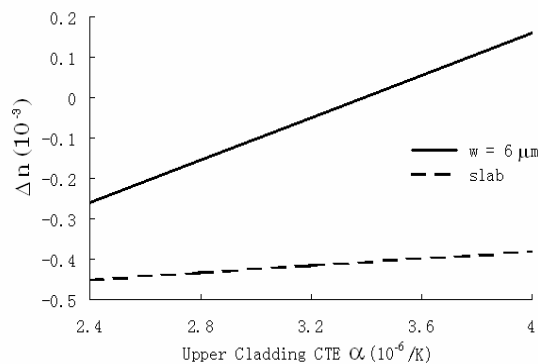


Fig. 1. Birefringence versus the thermal expansion coefficient of the upper cladding for a buried channel waveguide and a slab waveguide.

In a conventional AWG, the ends of the arrayed waveguides lie along a circular arc centered at the central input/output waveguide. As a result, the star couplers do not introduce any optical path length difference and therefore have no effect on the wavelength dispersion of the device. Only the arrayed waveguide region provides the optical path length difference. The basic diffraction equation for the central wavelength is:

$$n_a \Delta L = m \lambda_c \quad (1)$$

where n_a is the effective index of the arrayed waveguides, ΔL is the path length difference between adjacent arrayed waveguides, and m is the diffraction order. This leads to the polarization dependent wavelength shift $\Delta \lambda = \lambda_{TE} - \lambda_{TM} = (\Delta n_a / n_a) \lambda_c$, where $\Delta n_a = n_a(\text{TE}) - n_a(\text{TM})$ is the effective index difference (birefringence) of the arrayed waveguides.

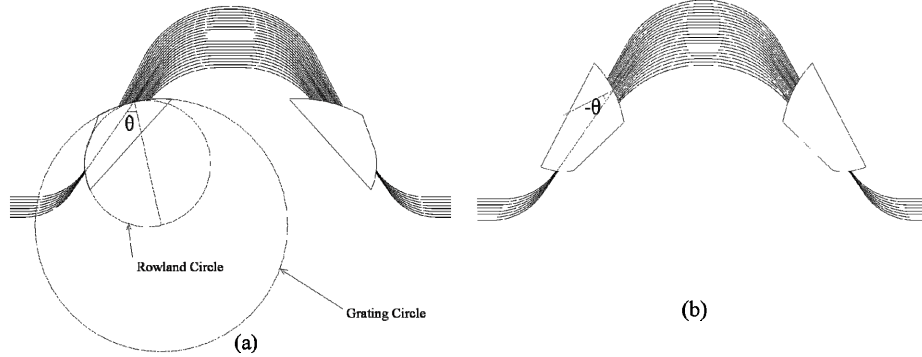


Fig. 2. Schematic of birefringence compensated AWGs with the same (a) and opposite (b) signs between the channel waveguide and the slab waveguide.

Since the birefringence of the slab waveguides of an AWG is generally different than that of the channel waveguides, as shown in Fig. 1, they can be compensated against each other by appropriately designing the shape of the star couplers. Figure 2 shows two example designs corresponding to a birefringence ratio of 1:3 with the same (a) and opposite (b) signs between the channel waveguide and the slab waveguide. The star couplers are designed according to Rowland circle construction with an oblique incident/diffraction angle θ (referred as the grating angle hereafter), similar to the case of an echelle grating [12]. The arrayed waveguides end at a grating circle while the ends of the input/output waveguides lie at a Rowland circle whose diameter is equal to the radius of the grating circle. The Rowland circle is tangent to the grating circle at the end of the central arrayed waveguide of the AWG, with the normal to the grating curve at the tangent point forming the grating angle θ with respect to the line connecting the central input/output waveguide and the central arrayed waveguide (the optical axis). When θ is zero, it becomes a conventional AWG. When θ is not zero, the total path length difference corresponding to adjacent arrayed waveguides is produced in both the slab region and the arrayed waveguide region. Consequently, the diffraction equation for the central wavelength becomes:

$$2n_s \Delta L_s + n_a \Delta L = m \lambda_c \quad (2)$$

where ΔL_s is the path length difference in the slab and n_s is the effective index of the slab waveguides. In this case, the polarization dependent wavelength shift becomes $\Delta \lambda = \lambda_{TE} - \lambda_{TM} = [(2\Delta n_s \Delta L_s + \Delta n_a \Delta L) / (2n_s \Delta L_s + n_a \Delta L)] \lambda_c$, where $\Delta n_s = n_s(\text{TE}) - n_s(\text{TM})$ is the effective index difference (birefringence) of the slab waveguides between the TE and TM modes. The condition for polarization insensitive operation, i.e. $\Delta \lambda = 0$, becomes

$$2\Delta n_s \Delta L_s + \Delta n_a \Delta L = 0 \quad (3)$$

Equations (2) and (3) determine the path length differences ΔL_s and ΔL , which in turn determine the grating angle θ and the AWG layout.

3. Design of the birefringence compensated AWGs

AWGs have many degrees of design freedom and a specific design approach has been given in Ref [13]. Our approach to birefringence compensated AWG design, in particular the design of the slab waveguide geometry, is described below.

Assume the number of channels N_{ch} , channel spacing $\Delta\lambda_{ch}$, and the central wavelength λ_c have been determined according to the application. The diffraction order of the AWG is then chosen according to the free spectral range (FSR) requirement, i.e. $FSR \approx \lambda_c/m > N_{ch}\Delta\lambda_{ch}$, where m is the diffraction order. In practice, m needs to be significantly smaller than $\lambda_c/(N_{ch}\Delta\lambda_{ch})$ in order to have a good channel non-uniformity. From the effective indices and the birefringence properties of the channel waveguide and the slab waveguide, the path length differences ΔL in the channel waveguides and ΔL_s in the slab waveguides are determined from Eqs. (2) and (3).

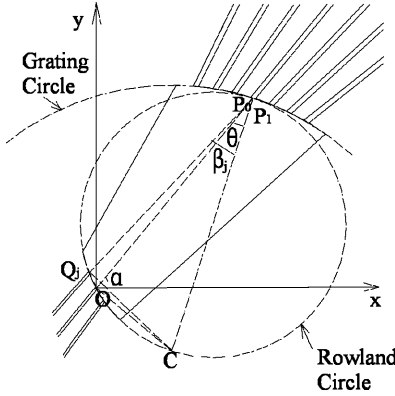


Fig. 3. Schematic diagram of the input star coupler.

Figure 3 is a schematic diagram of the input star coupler. For clarity, only a few waveguides are shown and the spacing is out of proportion. The origin O is the center of the central input waveguide. We denote the end points of the arrayed waveguides by P_i ($i=0, \pm 1, \pm 2, \dots$) with P_0 being the end of the central waveguide. Line OP_0 is therefore the optical axis, and its length is L_f . This length is chosen to be large enough to produce sufficient wavelength dispersion and make sure the loss non-uniformity of the AWG is acceptable (e.g. $<0.5\text{dB}$). Point C is the center of the grating circle. Its coordinates are determined by $x_c = L_f \tan\theta \sin\alpha$ and $y_c = -L_f \tan\theta \cos\alpha$, where α is the angle between the optical axis and the x axis.

Note that for an oblique grating angle, the ends of the arrayed waveguides are no longer disposed along the grating circle with equal spacing. We use the distance $d_a = P_0P_1$ between the end points of the central waveguide and its first adjacent waveguide ($i=1$) as an input design parameter. The insertion loss of the AWG is primarily caused by the interspaces among the arrayed waveguides. It decreases with decreasing d_a . However, because of fabrication limitations related to photolithography, dry etching and upper cladding deposition, these interspaces need to be larger than a minimum value (e.g. $1\sim 2\mu\text{m}$). Larger spacing also helps to mitigate phase errors due to the coupling between arrayed waveguides.

Once the length L_f of the star coupler, the angle α and the distance d_a are chosen, the slab geometry can be determined, including the end positions of the arrayed waveguides and the end positions of the input/output waveguides. From the principle of Rowland circle construction, we have

$$(x_{pi} - x_c)^2 + (y_{pi} - y_c)^2 = (L_f / \cos\theta)^2 \quad (4)$$

$$x_{pi}^2 + y_{pi}^2 = (L_f - i\Delta L_s)^2 \quad (5)$$

where (x_{pi}, y_{pi}) is the coordinates of the end position of the i^{th} arrayed waveguide. For $i=1$, we also have

$$(x_{p1} - x_{p0})^2 + (y_{p1} - y_{p0})^2 = d_a^2 \quad (6)$$

where $x_{p0} = L_f \cos \alpha$, $y_{p0} = L_f \sin \alpha$. After x_{p1} and y_{p1} are solved from Eqs. (5) and (6), the grating angle θ can be determined by the following equation derived from Eqs. (4) and (5)

$$\tan \theta = \frac{\Delta L_s (\Delta L_s - 2L_f)}{2L_f (x_{p1} \sin \alpha - y_{p1} \cos \alpha)} \quad (7)$$

The coordinates (x_{pi}, y_{pi}) of the end positions of the other arrayed waveguides ($i \neq 0, 1$) can then be obtained by solving Eqs. (4) and (5).

From Eq. (7), we can see that when $\Delta L_s = 0$, we have $\theta = 0$. In this case, the AWG becomes a conventional AWG. For some parameters (e.g. when the length difference ΔL_s in the slab region is too large), it is possible that the AWG cannot be constructed properly because θ is too large. This problem can be mitigated to a certain extent by reducing the diffraction order or increasing d_a (waveguide tapers can be used to reduce insertion loss). The diffraction order and d_a needs to be chosen appropriately so that θ is not too large. Usually, the grating angle θ should be less than 60 degrees, in order to avoid significant aberrations and unsatisfactory birefringence compensation, especially for edge channels.

The geometrical layout of the arrayed waveguides can be determined using similar method as in conventional AWG design. The end positions of the input/output waveguides are determined by the diffraction equation of the AWG. Consider the case where the light is input from the central input waveguide. The diffraction angle β_j for the wavelength λ_j satisfies:

$$n_s d_a \sin \theta + n_s d_a \sin \beta_j + n_a \Delta L = m \lambda_j \quad (8)$$

Since the ends of the output waveguides are disposed along the Rowland circle, their positions are determined after knowing the diffraction angle β_j for each wavelength channel. We denote the end points of the output waveguides by Q_j . The layout of the output star coupler is a mirror image of the input star coupler. For convenience, we overlap the notations for the output waveguides onto the input star coupler in Fig. 3. According to Rowland circle construction, the length of line $P_0 Q_j$ is $L_f \cos \beta_j / \cos \theta$ and the angle between the line $P_0 Q_j$ and the x axis is $\alpha - \beta_j + \theta$. The coordinates (x_{aj}, y_{aj}) of the end positions of the output waveguides can then be obtained by

$$x_{aj} = x_{p0} - L_f \cos \beta_j \cos(\alpha - \beta_j + \theta) / \cos \theta \quad (9)$$

$$y_{aj} = y_{p0} - L_f \cos \beta_j \sin(\alpha - \beta_j + \theta) / \cos \theta \quad (10)$$

The spacings between the output waveguides are not uniform and they need to be checked to make sure they are large enough for an acceptable crosstalk level. The parameters L_f and d_a can be adjusted for this purpose. The crosstalk due to coupling between adjacent waveguides can be calculated using overlap integral method. Since the channel passband is inversely proportional to the output waveguide spacing, a compromise need to be made between low crosstalk and wide passband. Passband flattening techniques can also be implemented similar to conventional AWG demultiplexers.

4. Simulation results and discussions

Two-dimensional beam propagation method (BPM) in combination with the effective index method (EIM) [14] is used to perform the numerical simulation. Figure 4(a) shows the spectral response of the central output waveguide for a conventional AWG with stress-induced birefringence. The birefringences of the slab waveguides and the arrayed waveguides are assumed to be -0.432×10^{-3} and -0.144×10^{-3} , respectively, corresponding to an upper cladding thermal expansion coefficient of $2.84 \times 10^{-6}/K$ [9] in Fig. 1. The $PD\lambda$ is about 0.15nm. Figure 4(b) shows the spectral response of the central channel for the birefringence compensated AWG. The TE and TM responses become completely overlapped. The parameters of the polarization compensated AWG are determined when both Eqs. (2) and (3)

are satisfied. The total device size is about 35mmx19mm in both cases. Table 1 gives other design parameters of the birefringence compensated AWG.

Since the path length difference in the output slab coupler is slightly dependent on the position of the output waveguides, the birefringence compensation is not perfect for edge channels. We have calculated the $PD\lambda$ for all the output waveguides of a 16-channel AWG, with the input light from the central input waveguide, as shown in Fig. 5. It is found that the $PD\lambda$ is less than 0.002nm for all wavelength channels.

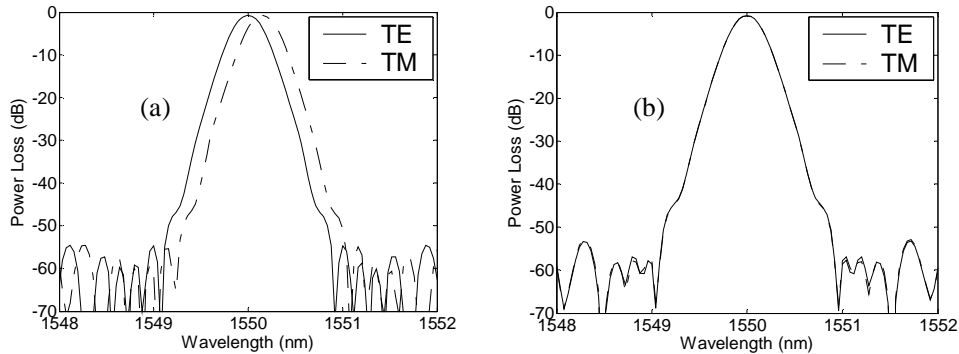


Fig. 4. Spectral response of the central output waveguide for AWGs with conventional (a) and angled (b) star couplers.

Table 1. Parameters of the birefringence compensated AWG

Central wavelength (nm)	1550.0
Diffraction order	45
Effective index of slab waveguides (TE)	1.452971
Birefringence of slab waveguides	-0.432×10^{-3}
Effective index of arrayed waveguides (TE)	1.450690
Birefringence of arrayed waveguides	-0.144×10^{-3}
Grating angle	50.367°
Slab Length (μm)	7000.0
Length difference in the arrayed waveguide region (μm)	72.18
Length difference in the slab region (μm)	-12.03

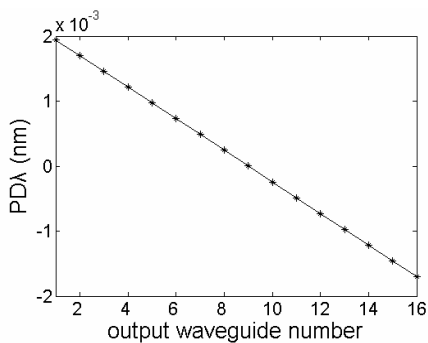


Fig. 5. $PD\lambda$ versus output waveguide number.

5. Summary

We have proposed a novel design for achieving birefringence compensation in AWGs. A more general and flexible AWG design with angled star couplers is introduced and simulation

results are presented. This method has the advantage of fabrication simplicity over previously reported techniques, and is applicable to various material systems with either stress induced or waveguide geometry induced birefringence.

Acknowledgments

This work was partially supported by Natural Science Foundation of Zhejiang Province (under grant No. X106875).